

Dense Hadronic Matter in Neutron Stars*

LAURA TOLOS

Institute of Space Sciences (ICE, CSIC), Campus UAB, Carrer de Can Magrans,
08193, Barcelona, Spain;

Institut d'Estudis Espacials de Catalunya (IEEC), 08034 Barcelona, Spain;

Frankfurt Institute for Advanced Studies, University of Frankfurt,

Ruth-Moufang-Str. 1, 60438 Frankfurt am Main, Germany

In this lecture we discuss the properties of dense hadronic matter inside neutron stars. In particular, we pay attention to the role of strangeness in the core of neutron stars, by analysing the presence of baryons and mesons with strangeness. We consider two interesting possible scenarios in their interior, that is, the existence of hyperons leading to the so-called hyperon puzzle and the presence of a kaon condensed phase inside neutron stars.

1. A short introduction to neutron stars

Neutron stars (NSs) are an excellent laboratory to study the properties of matter under extreme conditions of density, isospin asymmetry and temperature as well as in the presence of strong gravitational and magnetic fields.

NSs are the final product of core-collapse supernovae. They are in hydrostatic equilibrium with the gravitational collapse mainly counterbalanced by the neutron degeneracy pressure. NSs usually have masses around 1-2 M_{\odot} and radii about 10-12 km, that leads to average densities of $\sim 10^{14}$ g/cm³, hence, to very compact stellar objects. However, these stars show an onion-like configuration, where densities extend over a large range. A diagrammatic representation of their internal structure is shown in Fig. 1, where several layers can be seen, that is, the atmosphere; the outer and inner crust, with ≈ 1 km; and the core, splitted in the outer and inner core, with a radius of ≈ 10 km which contains almost the total mass of the NS.

In spite of the fact that the inner region of an NS is the largest part and, therefore, the one that determines the properties of an NS, its composition is

* Presented at the LXIII Cracow School of Theoretical Physics Nuclear Matter at Extreme Densities and High Temperatures, Zakopane, Poland, 17–23 September, 2023.

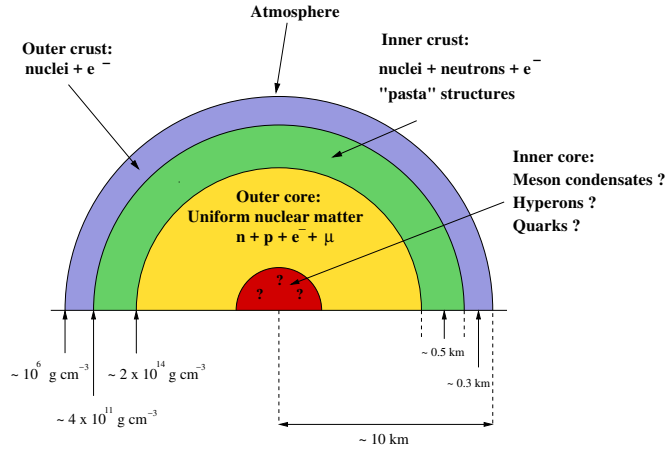


Fig. 1. Illustrative representation of the interior of a neutron star. Figure adapted from Ref. [1] and taken from Ref. [2].

not known. Thus, several hypothesis have been put forward. These include the presence of matter made of hadrons, such as baryons or mesons, and/or the existence of deconfined quark matter.

In this lecture we aim at describing the properties of hadronic matter inside NSs and the consequences for the structure of these compact objects, paying a special attention to the role of strangeness in the interior of NSs. We refer the reader to [2, 3, 4] for recent reviews on dense matter in NSs.

We start by assuming baryonic matter inside NSs. NSs are charged neutral objects equilibrated by weak interaction processes, that is, they are in β -equilibrium. This equilibrium can be expressed as

$$b_1 \rightarrow b_2 + l + \bar{\nu}_l, \quad b_2 + l \rightarrow b_1 + \nu_l, \quad (1)$$

where b_i refers to a certain type of baryon, l represents a lepton, and ν_l and $\bar{\nu}_l$ are the corresponding neutrino and antineutrino, respectively. The composition of the interior of NSs is determined by studying all the possible weak reactions among the different species inside the core. This can be expressed by means of the particle chemical potentials μ_i , such as

$$\begin{aligned} \mu_{b_i} &= B_{b_i} \mu_n - q_{b_i} \mu_e, \\ \mu_{l_j} &= -q_{l_j} \mu_e, \end{aligned} \quad (2)$$

where B_{b_i} is the baryonic number of a given baryon b_i , $q_{b_i(l_j)}$ is the charge of b_i baryon (l_j lepton), and μ_n and μ_e are the chemical potentials of the neutron and electron, respectively. We note that (anti-)neutrinos freely

escape without contributing to the energy balance as their mean-free path is larger than the typical size of an NS.

The charged neutrality is guaranteed by

$$\sum_{b_i} q_{b_i} \rho_{b_i} + \sum_{l_j} q_{l_j} \rho_{l_j} = 0, \quad (3)$$

where $\rho_{b_i(l_j)}$ is the density of $b_i(l_j)$, with the total baryonic density given by

$$\rho = \sum_{b_i} B_{b_i} \rho_{b_i}. \quad (4)$$

In order to connect the microphysics to the bulk properties of an NS, specifically the mass and radius of an NS, we need to solve the so-called structure equations for NSs. These can be determined by means of Einstein's general relativity theory. In the case of a spherical static star, the Einstein's field equations become the Tolman-Oppenheimer-Volkoff (TOV) structure equations¹:

$$\frac{dP(r)}{dr} = -\frac{1}{r^2} [\varepsilon(r) + P(r)] [M(r) + 4\pi r^3 P(r)] \left[1 - \frac{2M(r)}{r}\right]^{-1}, \quad (5)$$

$$\frac{dM(r)}{dr} = 4\pi r^2 \varepsilon(r). \quad (6)$$

where we have used $G = c = 1$ units.

The TOVs are a set of coupled equations that describe the hydrostatic equilibrium obtained in general relativity. Their interpretation is straightforward. From Eq. (6), the mass energy of a shell of matter of radius r and thickness dr can be obtained. As for the left-hand side of Eq. (5), this is related to the net force acting outwards on the surface of the shell by the pressure difference between the interior and the exterior, $dP(r)$, while the right-hand side of this equation comes from the force of gravity acting on the shell due to the mass accumulated in the interior.

In order to solve the TOVs, we need to determine the pressure P and the associated energy density ε for a given composition of the interior of the NS, that is, we need to obtain the so-called equation of state (EoS). Once the EoS is fixed, the TOV equations can be integrated by fixing the initial conditions to the enclosed mass and the pressure at the center of the NS, $M(r=0) = 0$ and $P(r=0) = P_c$, with P_c taking an arbitrary value

¹ We note that NSs are usually detected as pulsars, that is, rotating stars. Therefore, the spherical symmetry is broken and the axial symmetry is the only symmetry remaining as NSs flatten with rotation. This leads to study rotating NSs with a perturbative method developed by Hartle and Thorne [5].

from the EoS. The integration over the radial coordinate r finishes when $P(r = R) = 0$, with R being the radius and $M(R)$ the total mass M of the star, respectively.

2. The nuclear equation of state

As we mentioned earlier, the gravitational collapse of NS is mainly counterbalanced by the neutron degeneracy pressure. Thus, one of the first hypothesis for baryonic matter would be to consider the interior of NSs as a neutron Fermi gas. However, this is a very unrealistic scenario. On the one hand, an NS must contain a small fraction of protons and electrons so as to inhibit neutrons from decaying into protons and electrons by their weak interactions. On the other hand, the Fermi gas model ignores nuclear interactions, which give important contributions to the energy density. Therefore, we start by assuming that the core of an NS is made of nuclear matter.

The EoS of nuclear matter describes an idealised infinite uniform system made of nucleons (protons and neutrons), where the Coulomb interaction is switched off. Symmetric nuclear matter refers to a system with an equal number of neutrons and protons, and is the easiest approximation to bulk matter in heavy atomic nuclei. Pure neutron matter, on the other hand, is the simplest approach to hadronic matter in the NS core.

The energy per nucleon of the nuclear system for a given density ρ can be expressed as

$$\frac{E}{A}(\rho, \delta) = \frac{E}{A}(\rho, 0) + S(\rho)\delta^2 + \dots, \quad (7)$$

with $\delta = (N - Z)/A$ and $A = N + Z$, being $N(Z)$ the neutron (proton) number. The energy per nucleon of symmetric nuclear matter ($\delta = 0$) is given by $(E/A)(\rho, 0)$, while $S(\rho)$ is the symmetry energy that measures the energy cost involved in changing the protons into neutrons. If we expand both terms around nuclear saturation density, ρ_0 , we obtain

$$\begin{aligned} \frac{E}{A}(\rho, 0) &= \frac{E}{A}(\rho_0) + \frac{1}{18}K_0\epsilon^2 + \dots, \\ S(\rho) &= S_0 + \frac{1}{3}L\epsilon + \frac{1}{18}K_{\text{sym}}\epsilon^2 + \dots, \end{aligned} \quad (8)$$

where $\epsilon = (\rho - \rho_0)/\rho_0$. The binding energy per nucleon at saturation density, $(E/A)(\rho_0)$, and the incompressibility at the saturation point, K_0 , are called isoscalar parameters, whether the symmetry energy coefficient at saturation density, S_0 , and L and K_{sym} , that give the density dependence of the symmetry energy around saturation, are usually referred as isovector

parameters. These parameters are given by

$$\begin{aligned}
 K_0 &\equiv 9\rho_0^2 \left(\frac{\partial^2(E/A)(\rho, \delta)}{\partial \rho^2} \right)_{\rho_0, \delta=0}, & S_0 &\equiv \frac{1}{2} \left(\frac{\partial^2(E/A)(\rho, \delta)}{\partial \delta^2} \right)_{\rho_0, \delta=0}, \\
 L &\equiv 3\rho_0 \left(\frac{\partial S(\rho)}{\partial \rho} \right)_{\rho_0}, & K_{\text{sym}} &\equiv 9\rho_0^2 \left(\frac{\partial^2 S(\rho)}{\partial \rho^2} \right)_{\rho_0}.
 \end{aligned} \tag{9}$$

The energy density of the system $\varepsilon(\rho, \delta)$ and the pressure P are straightforwardly obtained by

$$\begin{aligned}
 \varepsilon(\rho, \delta) &= \rho \frac{E}{A}(\rho, \delta), \\
 P(\rho, \delta) &= \rho^2 \frac{\partial(E/A)(\rho, \delta)}{\partial \rho} = \rho \frac{\partial \varepsilon(\rho, \delta)}{\partial \rho} - \varepsilon(\rho, \delta).
 \end{aligned} \tag{10}$$

2.1. Constraints on the nuclear equation of state

Several constraints on the nuclear EoS can be obtained from nuclear experiments and/or observations. Nonetheless, we have to take several of these constraints with caution since they are determined after using theoretical modelling and/or by means of extrapolations to domains not attainable by experiments and/or observations. In this section we present some experimental and observational constraints that are usually considered for constraining the nuclear EoS.

2.1.1. Constraints from nuclear experiments

Several constraints on the isoscalar and isovector parameters can be extracted from nuclear experiments.

With regard to the previously mentioned isoscalar parameters of the nuclear EoS, the values for the nuclear saturation density $\rho_0 = 0.15 - 0.16 \text{ fm}^{-3}$ and the binding energy per nucleon at that density $(E/A)(\rho_0) = -16 \pm 1 \text{ MeV}$ have been determined from the measurement of density distribution [6] and nuclear masses [7]. As for the incompressibility at saturation density K_0 , the extraction of its value is complicated and results have a wide spread of $K_0 \sim 200\text{-}300 \text{ MeV}$ (see for example [8, 9, 10]).

As for the isovector parameters S_0 , L and K_{sym} , these can be extracted from experiments involving isospin diffusion measurements [11], analysis of giant [12] and pygmy resonances [13, 14], isobaric analog states [15], isoscaling [16], production of pions [17] and kaons [18, 19, 20] in heavy-ion collisions (HiCs) or data on neutron skin thickness of heavy nuclei [21, 22, 23, 24]. Whereas S_0 is relatively well constrained around $\sim 30 \text{ MeV}$, L and K_{sym} are still poorly known.

2.1.2. Constraints from neutron star observations

Other sources to constrain the nuclear EoS come from NS observations, such as masses and radii, and more recently from gravitational wave detection.

The mass of an NS can be determined if the NS is located in a binary system by means of using the Kepler's law modified by general relativity effects. In binary systems, there exist five Keplerian (also called orbital parameters) that can be measured with good precision. These are the binary orbital period (P_b), the orbit's eccentricity (e), the projection of the semi-major axis onto the line of sight ($x \equiv a_1 \sin i$, with i being the inclination angle of the orbit), and the time of the periastron (T_0) and its longitude (ω_0). Using Kepler's law, the so-called mass function can be obtained. This is a relation between the masses of both stars and some of the observed orbital parameters, that is, $f(M_P, M_C, i) = M_c^3 \sin^3 i / (M_P + M_C)^2 = 4\pi^2 x^3 / P_b^2$, with M_P representing the mass of the NS ($P =$ pulsar) and M_C being the mass of its companion.

In order to determine both masses, we need more information. We then resort to determine the deviations from the Keplerian orbit due to general relativity effects. These effects can be described by the so-called post-Keplerian parameters. These post-Keplerian parameters are the advance of the periastron ($\dot{\omega}$), the changes in the transverse Doppler shift together with the gravitational redshift around an elliptical orbit (γ), the range (r) and shape (s) of the Shapiro time delay, and the orbital decay (\dot{P}_b). We note that the post-Keplerian parameters are dependent on the Keplerian parameters and the two masses in the binary. Therefore, if we could determine at least two of them as well as the mass function, we could obtain the masses of the two stars. The further determination of a third post-Keplerian parameter will result in a test of general relativity.

Nowadays more than 2000 pulsars have been discovered, with some of their masses very well determined. The detection and measurement of the masses of the Hulse-Taylor pulsar and its companion [25] result in the Nobel Prize in 1993 for Hulse and Taylor, because it allowed to a test Einstein's general relativity. More recent accurate values of $2M_\odot$ have been reported, such as for the PSR J1614-2230 [26, 27], the PSR J0348+0432 [28], and the PSR J0740+6620 of $2.14_{-0.09}^{+0.10} M_\odot$ [29]. As we will later discuss, these $2M_\odot$ measurements are sometimes in tension with theoretical predictions for EoSs that take into account the presence of hyperons.

With regard to radii, these were extracted from studying the X-ray spectra emitted by the NS atmosphere. This is a rather difficult task as the X-ray spectra strongly depends on the distance to the star, its magnetic field and the composition of the atmosphere. However, very recently, the situa-

tion has dramatically improved with space missions such as NICER (Neutron star Interior Composition ExploreR) [30], and the future STROBE-X (Spectroscopic Time-Resolving Observatory for Broadband Energy X-rays) [31] and eXTP (enhanced X-ray Timing and Polarimetry) [32], since high-precision X-ray astronomy offers precise determinations of masses and radii in a simultaneous way. Simultaneous measurements of masses and radii are already becoming available from NICER, with the first precise measurements of the radii and masses of the millisecond pulsars PSR J0030+0451 and PSR J0740+6620 [33, 34, 35, 36].

Furthermore, the detection of gravitational waves coming from the merger of two NSs by the LIGO and VIRGO collaborations [37, 38] has opened new frontiers. Gravitational waves from the late inspirals of NSs depend on the EoS, via the so-called tidal deformability. Indeed, the tidal deformability depends on the NS compactness. Therefore, the measurement of the tidal deformability helps to constrain the EoS.

2.2. Theoretical models for the nuclear equation of state

Nuclear matter inside the core of an NS can be described by means of different theoretical many-body approaches, that are usually classified between microscopic ab-initio schemes and phenomenological approaches.

Microscopic ab-initio approaches refer to schemes where the nuclear EoS is obtained by solving the many-body problem from two-nucleon (NN) and three-nucleon interactions (NNN). These NN and NNN interactions are fitted to scattering data and finite nuclei. These schemes include the ones based on the variational analysis [39], quantum-montecarlo methods [40, 41, 42], the formalism of the correlated basis function [43], diagrammatic approaches (among them, the Brueckner-Bethe-Goldstone expansion [44], the Dirac-Brueckner-Hartree-Fock (DBHF) method [45, 46] and the self-consistent Green's function scheme [47]), renormalization group methods [48], and lattice Quantum Chromodynamics (LQCD) computations [49, 50]. Whereas the advantage of the vast majority of these approaches is being able to systematically add higher-order contributions that allows for a controlled determination of the nuclear EoS, the main disadvantage lies on the applicability to large densities, since incorporating higher-order terms makes the computations more difficult.

Phenomenological schemes are based on interactions that depend on the density and are adjusted to nuclear observables and observations coming from NSs. Among others, we have non-relativistic energy-density functionals, such as the Skyrme [51] or Gogny [52] approaches, or relativistic models, usually derived from an hadronic Lagrangian, using the mean-field or Hartree-Fock approximations [53, 54]. The clear advantage of these ap-

proaches is the applicability to large densities, while the disadvantage lies on the non-systematic character of these approaches.

For more details on these approaches, we refer to the recent works of Refs. [4, 55, 56].

3. Equation of state with strangeness

Given the extreme density conditions inside NSs as compared to those found on Earth, the existence of new phases of matter in their interior is therefore possible. In particular, the presence of strange baryons (also called hyperons) and strange mesons (antikaons) in the interior of NSs has been explored extensively over the years. In this section we aim at describing strange hadronic matter and the consequences for the structure of NSs. In particular, we will discuss the so-called hyperon puzzle and the phenomenon of kaon condensation in NSs.

3.1. Strange baryons: Hyperons

Hyperons are baryons with one or more strange quarks. They are usually denoted by Y and refer to Λ , Σ and Ξ . In this part of the lecture we aim at describing the role of hyperons inside NSs. To that end, we first start by summarizing the present experimental status of the YN and YY interactions, followed by shortly describing several theoretical approaches for the YN and YY interactions. We continue by analyzing the properties of hyperons in a many-body baryonic system, and finally address the presence of hyperons in NSs and the hyperon puzzle.

3.1.1. Experimental status for YN and YY interactions

In contrast to the NN system, the YN and YY interactions are poorly constrained. The experimental difficulties arise from the short life of hyperons together with the low-density beam fluxes. Whereas for the ΛN and ΣN systems there are hundred of scattering events [57, 58, 59, 60, 61], few exist for ΞN system and non scattering data is available for YY .

Alternatively, the study of hypernuclei, that is, bound systems composed of nucleons and one or more hyperons can give us information on the YN and YY interactions. More than 40 single Λ -hypernuclei, and a few double- Λ and single- Ξ ones have been detected. As for Σ hypernuclei the experimental confirmation is ambiguous, indicating that the ΣN interaction is most probably repulsive. For a short review on hypernuclei, we refer to Ref. [62].

More recently, femtoscopy has emerged as a very interesting tool to study reactions among hadrons [63]. Femtoscopy consists in measuring the

hadron-hadron correlation in momentum space by obtaining the ratio of the distribution of relative momenta for pairs produced in the same collision and in different collisions (mixed events). If the measured correlation is larger than one, the interaction is attractive, whereas the values are between zero and one if the interaction is repulsive or a bound state exists. Thus, the comparison of the measured correlation functions with the theoretical predictions will give us information on hadron-hadron interactions, and in particular, on the YN and YY interactions.

3.1.2. Theoretical approaches to YN and YY interactions

In the past there has been a lot of theoretical progress trying to describe the YN and YY interactions. The theoretical schemes can be grouped in meson-exchange schemes, chiral effective field theory (χ EFT) approaches, calculations on LQCD, low-momentum schemes and quark-model potentials.

The basic idea in meson-exchange models is that the interaction between two baryons is mediated by the exchange of mesons. Starting from the NN meson-exchange model, $SU(6)_{\text{flavor}}$ symmetry is assumed to obtain the YN and YY interactions in the Jülich [64] potential, whereas $SU(3)_{\text{flavor}}$ symmetry for the Nijmegen [65] ones.

As for the χ EFT schemes, the YN and YY interactions have been built by the Jülich-Bonn-Munich group starting from their previous NN χ EFT approach [66, 67, 68].

Regards to LQCD, the QCD path integral over the quark and gluon fields at each point of a four-dimensional space-time grid is solved by means of Monte Carlo techniques. HALQCD [69] and the NPLQCD [70] collaborations are pioneers in this respect.

And, finally, the YN and YY interactions have been described using other schemes that include low-momentum interactions and quark-model potentials. The former determines a universal effective low-momentum potential for YN and YY using renormalization-group methods [71], whereas the latter builds the YN and YY interactions within constituent quark models [72].

3.1.3. Hyperons in dense matter

The properties of hyperons in dense matter can be obtained from YN and YY interactions by means of incorporating corrections from the surrounding many-body medium. Within this microscopic formulation, one of the most used scheme is the Brueckner-Hartree-Fock (BHF) approach to calculate single-particle potentials of hyperons in dense nuclear matter. The

starting point of this approach is the use the NN, YN and YY potentials, supplemented by three-body forces.

Whereas initial works on BHF computations were based on the Jülich and Nijmegen meson-exchange potentials, more recently the single-particle potentials for hyperons have been obtained with the χ EFT approaches. Within these schemes, the Λ and Σ single-particle potentials have been computed [73, 74]. The Σ -nuclear potential is found to be repulsive, whereas the Λ single-particle potential is in good qualitative agreement with the empirical values extracted from hypernuclear data, becoming repulsive about two to three-times saturation density. As for the Ξ single-particle potential in nuclear matter, values ranging between -3 to -5 MeV are determined, whereas the reported experimental value is larger.

The effect of three-body forces has been also studied, in particular for the case of the Λ -nuclear interaction [75]. The inclusion of the three-body forces is important for obtaining binding energies of few nucleons, scattering observables and the nuclear saturation properties in non-relativistic schemes, such as BHF. The implementation of three-body forces for the Λ -nuclear interaction in dense matter gives an extra repulsion at large densities, that could be relevant for the presence of hyperons in NSs [76, 77], as we will discuss in the next section.

3.1.4. Hyperons inside neutron stars: the hyperon puzzle

As previously mentioned, a realistic scenario inside NSs involves the presence of neutrons and protons interacting, as well as electrons via weak equilibrium reactions when nucleons are involved². However, more exotic degrees of freedom could be also expected in the core of an NS.

Hyperons in NSs were first taken into consideration in the seminal work of Ref. [78]. Ever since, the presence of hyperons in the interior of NSs have been thoroughly studied (for recent reviews see [2, 4, 62, 79]). Hyperons may appear inside NSs at densities of $\approx 2\text{-}3\rho_0$. This is due to the fact that the nucleon chemical potential could be so large at these densities so that it is energetically more favourable to have hyperons than nucleons. As a result, the EoS becomes softer as the system relieves Fermi pressure, as observed in the left panel of Fig. 2. If the EoS becomes softer, then there is less pressure inside an NS, and, hence, the NS has less mass, as shown in the right panel of Fig. 2. The softening of the EoS may then lead to maximum masses not compatible with the $2M_\odot$ measurements, such as the masses of the PSR J1614-2230 [26, 27], PSR J0348+0432 [28] and PSR J0740+6620 [29], as seen in the right panel of Fig. 2. This fact is usually referred as

² We have not explicitly mentioned the existence of muons, but those can be also present when nucleons are considered.

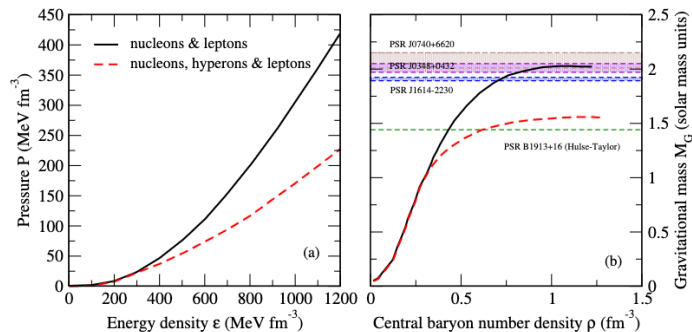


Fig. 2. The EoS (left panel) and the corresponding NS mass (right panel), without (black solid lines) and with (red dashed lines) hyperons. The mass of the Hulse-Taylor pulsar and the masses of PSR J1614-2230 [26, 27], PSR J0348+0432 [28] and PSR J0740+6620 [29] are shown with horizontal lines. Figure taken from Ref. [80].

the hyperon puzzle, and several solutions have been put forward in order to have hyperons in the interior of $2M_{\odot}$ NSs. Here we briefly comment on them.

One solution to the hyperon puzzle takes into account stiff YN and YY interactions (see, for example, [81, 82, 83, 84]). In this manner, the softening due to the presence of hyperons is overcome, thus reaching $2M_{\odot}$. Another possible way of solving the puzzle is given by the stiffening of the EoS thanks to hyperonic three-body forces. The hyperonic three-body forces give an additional repulsion at large densities so the EoS becomes stiff enough in order to be able to obtain $2M_{\odot}$ stars [75, 76, 77, 85, 86, 87, 88, 89, 90]. However, no general consensus has been reached. Other solutions consider the appearance of new species that could push the presence of hyperons to larger densities, such as Δ baryons [91, 92, 93] or a kaon condensed phase (see discussion on kaon condensation in the next section). Moreover, solutions based on the appearance of non-hadronic degrees of freedom have been taken into account, such as an early phase transition to quark matter below the hyperon onset (see Refs. [94, 95, 96, 97, 98] for recent papers). And, finally, more exotic solutions have been put forward, such as the use of modified gravity to accommodate hyperons inside $2M_{\odot}$ stars [99].

3.2. Strange mesons: Antikaons

Up to now we have assumed that hadronic matter is made of baryons. However, another possible scenario inside NSs is the presence of bosonic matter, in particular, the presence of strange mesons (antikaons denoted by \bar{K}) in the core of NSs. In order to fully understand the plausibility of having strange mesons in the interior of NSs, we should first address the interaction of strange mesons with dense matter and how the properties of strange mesons are modified in a dense medium.

Therefore, in this section we start by analysing the $\bar{K}N$ interaction and the role of the $\Lambda(1405)$ resonance. Afterwards, we address the interaction of strange mesons in a many-body system of nucleons. We continue by examining the role of strange mesons in HiCs, where a dense medium is produced. And, finally, we discuss the presence of antikaons in NSs, and the phenomenon of kaon condensation.

3.2.1. The $\bar{K}N$ interaction: the $\Lambda(1405)$

The $\bar{K}N$ interaction is governed by the presence of the $\Lambda(1405)$ state, which is a strange resonance with isospin $I = 0$, spin and parity $J^P = 1/2^-$ and strangeness $S = -1$. The $\Lambda(1405)$ was predicted to be of molecular type more than 50 years ago by Dalitz and Tuan [100, 101]. Since then, a lot of effort has been invested to understand its nature and, hence, the role of this state in the $\bar{K}N$ interaction. Several theoretical approaches have been used over the years, that include coupled-channel unitarized theories using meson-exchange models [102, 103] or meson-baryon χEFT [104, 105, 106, 107, 108, 109, 110, 111, 112]. Interestingly, these works conclude that the dynamics of the $\Lambda(1405)$ is described by the superposition of two states, between the $\bar{K}N$ and $\pi\Sigma$ thresholds [106, 109, 113], that can be seen experimentally in reaction-dependent line shapes [109].

3.2.2. Antikaons in matter

Once we know the features of the $\bar{K}N$ interaction, we can then address the interaction of antikaons in a many-body system of nucleons. Over the last decades antikaons in nuclear matter have been extensively analyzed. The first works used relativistic mean-field models (RMF) [114] or quark-meson coupling schemes [115] to obtain very large antikaon potentials of a few hundreds of MeVs at saturation density ρ_0 . Nevertheless, the doubtful assumption of the low-density theorem led these works to determine such a large \bar{K} potential in dense matter. The need of a description of the $\bar{K}N$ interaction taking into the $\Lambda(1405)$ in matter is essential.

One possible manner to proceed is by using unitarized theories in coupled channels in dense nuclear matter, based on χEFT [116, 117, 118] or

from meson-exchange schemes [119, 120], in both cases including the strange degree of freedom. Different effects have to be taken into account to fully determine the behaviour of the $\Lambda(1405)$ in dense matter and, hence, the medium modified $\bar{K}N$ interaction. Those are: i) the implementation of Pauli blocking on baryons in the intermediate meson-baryon propagator [121]; ii) the inclusion of the \bar{K} potential (or self-energy) in the \bar{K} propagation in dense matter [117]; and iii) the incorporation of self-energies of all hadrons in the intermediate states [118]. Within these schemes, an attractive antikaon potential is obtained with values below 100 MeV at saturation density. Moreover, the potential shows a considerable imaginary part, that is, the antikaon develops an important width because of the appearance of new decay channels of the antikaon in matter.

3.2.3. Experiments and observations: heavy-ion collisions

A possible scenario to analyze the interaction of antikaons with a dense system and, hence, extract information on the antikaon potential is to study the creation and propagation of antikaons in HiCs for intermediate beam kinetic energies (GeV). This analysis, however, requires the use of transport schemes to fully model the collisions. Transport models can be understood as the link between the experiments and the physical processes, since they consider the production and propagation of all kind of species, such as strange mesons (see Ref. [19] for a review on strangeness production). These schemes solve semi-classical transport equations of the Boltzmann-type, coming from non-equilibrium quantum field theory.

First transport calculations for antikaons in matter were performed neglecting the finite width of the antikaon potential in dense matter [122, 123]. Later on, the antikaon production was determined by means of off-shell dynamics with full in-medium antikaon properties within the Hadron-String-Dynamics (HSD) transport model [124]. In this case, the $\bar{K}N$ interaction in dense matter was obtained from the Jülich meson-exchange model [119, 120]. Recently, strangeness production in HICs at (sub-)threshold energies of 1 - 2 AGeV based on the microscopic Parton-Hadron-String Dynamics (PHSD) transport approach has been studied, considering the in-medium antikaon properties from the χEFT approach of Refs. [125, 126, 127]. Several experimental observables that involved strange mesons have been analyzed, such as rapidity distributions, p_T -spectra, the polar and azimuthal angular distributions, and directed and elliptic flow in C+C, Ni+Ni, and Au+Au collisions. The comparison of this analysis with the experimental data from the KaoS, FOPI and HADES Collaborations lead to the conclusion that the modifications of the strange meson properties in dense nuclear matter are necessary to explain the data consistently [20].

3.2.4. Experiments and observations: kaon condensation in neutron stars

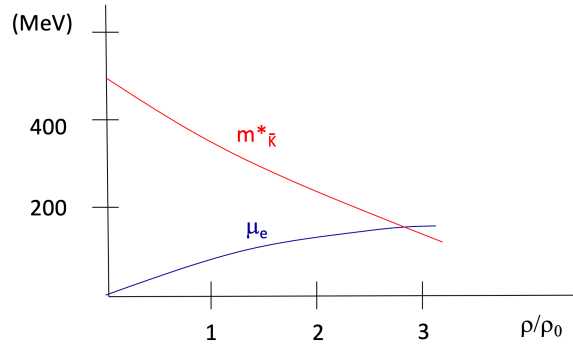


Fig. 3. Illustrative picture depicting the evolution of the electron chemical potential μ_e and the antikaon effective mass $m_{\bar{K}}^*$ with baryon density in the interior of NSs. Taken from Ref. [2].

The presence of antikaons is another possible scenario inside the core of NSs. As mentioned earlier, the composition of matter in NSs is found by demanding equilibrium against weak interaction processes. In particular, for matter composed of neutrons, protons and electrons, the weak interaction transitions are given by



with $\mu_n = \mu_p + \mu_e$ and $\rho_p = \rho_e$, with $\rho = \rho_p + \rho_n$. However, if the chemical potential of the electron substantially increases with density in the interior of an NS, antikaons might be produced instead of electrons as the following weak reactions could become energetically more favourable



In order for these reactions to take place, the chemical potential of the electron for a given density in the core of an NS should be larger than the effective mass of antikaons at that density, that means, $\mu_e > m_{\bar{K}}^*$. If this is the case, the phenomenon of kaon condensation would take place as antikaons would appear and form a condensed medium.

The possible existence of kaon condensation in NSs was considered in the pioneering work of Ref. [128]. The question that needs to be answered is whether the mass of antikaons could be largely modified in the nuclear

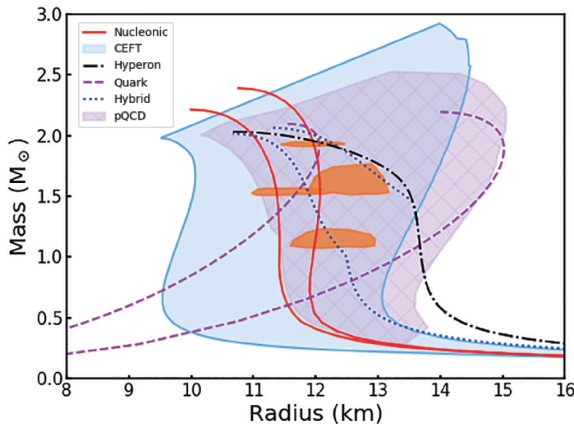


Fig. 4. Constraints from pulse profile modelling of rotation-powered pulsars with eXTP. Figure adapted from Ref. [32] and taken from Ref. [2].

medium. This is the case of some phenomenological schemes, in particular those based in RMF models (see, for example, the recent results in Refs. [129, 130, 131, 132]). However, the large modification in the mass of antikaons embedded in a nuclear medium is not obtained in microscopic unitarized schemes (see, for example, Refs. [117, 118, 119, 120, 125, 126, 127, 133]).

4. Conclusions and Outlook

In this lecture we have considered the properties of strange hadronic matter in a dense medium and, more precisely, inside NSs. In particular, we have discussed two possible scenarios in the interior of NSs, that is, the presence of hyperons which might lead to the hyperon puzzle and the phenomenon of kaon condensation.

To finalize we would like to discuss the future venue to address strange matter inside NSs through X-ray observations. In Fig. 4 we show the mass-radius diagram for NSs taking into account different possible scenarios inside NSs, together with constraints from pulse profile modelling with eXTP [32]. The expected constraints from pulse profile modelling of rotation-powered pulsars with eXTP are shown with the orange error contours for PSR J1614-2230 [26, 27], PSR J2222-0137 [134], PSR J0751+1807 [135] and PSR J1909-3744 [135]), whose masses are known precisely. The EoS mod-

els³ include nucleons (models AP3 and AP4) [39], quarks (u,d,s quarks) [139, 140], nucleons and hyperons (inner core with nucleons and hyperons, outer core with only nucleons) [81], or quarks and nucleons giving rise to hybrid stars (inner core of quarks, outer core of nucleons)[98]. The CEFT region shows the range of the nucleonic χ EFT EoS [141], while the pQCD domain results from interpolating CEFT at low densities and matching to perturbative QCD (pQCD) computations at higher densities [142].

From this figure it is clear the need of having precise simultaneous mass-radius observations to disentangle between the theoretical predictions for different types of dense matter inside NSs. Nonetheless, other observations are very much welcome, such as those coming from gravitational wave emission of NS binary mergers.

Acknowledgments

L.T. acknowledges support from CEX2020-001058-M (Unidad de Excelencia ‘‘María de Maeztu’’), PID2019-110165GB-I00 and PID2022-139427NB-I00 financed by the Spanish MCIN/AEI/10.13039/501100011033/FEDER, UE as well as from the Generalitat de Catalunya under contract 2021 SGR 171, by the EU STRONG-2020 project, under the program H2020-INFRAIA-2018-1 grant agreement no. 824093, and by the CRC-TR 211 ‘Strong-interaction matter under extreme conditions’- project Nr. 315477589 - TRR 211.

REFERENCES

- [1] I. Vidaña. A short walk through the physics of neutron stars. *Eur. Phys. J. Plus*, 133(10):445, 2018.
- [2] L. Tolos and L. Fabbietti. Strangeness in Nuclei and Neutron Stars. *Prog. Part. Nucl. Phys.*, 112:103770, 2020.
- [3] A. L. Watts et al. Colloquium: Measuring the neutron star equation of state using X-ray timing. *Rev. Mod. Phys.*, 88(2):021001, 2016.
- [4] G. F. Burgio, H. J. Schulze, I. Vidana, and J. B. Wei. Neutron stars and the nuclear equation of state. *Prog. Part. Nucl. Phys.*, 120:103879, 2021.
- [5] J. B. Hartle and K. S. Thorne. Slowly Rotating Relativistic Stars. II. Models for Neutron Stars and Supermassive Stars. *Astrophys. J.*, 153:807, 1968.
- [6] H. De Vries, C. W. De Jager, and C. De Vries. Nuclear charge and magnetization density distribution parameters from elastic electron scattering. *Atom. Data Nucl. Data Tabl.*, 36:495–536, 1987.

³ We note the existence of the online service ComPOSE repository that provides data tables for different state of the art EoSs ready for use in astrophysical applications, nuclear physics and beyond [136, 137, 138].

- [7] G. Audi, A.H. Wapstra, and C. Thibault. The ame2003 atomic mass evaluation: (ii). tables, graphs and references. *Nuclear Physics A*, 729(1):337–676, 2003. The 2003 NUBASE and Atomic Mass Evaluations.
- [8] J. P. Blaizot. Nuclear Compressibilities. *Phys. Rept.*, 64:171–248, 1980.
- [9] J. Piekarewicz. Unmasking the nuclear matter equation of state. *Phys. Rev.*, C69:041301, 2004.
- [10] E. Khan and J. Margueron. Constraining the nuclear equation of state at subsaturation densities. *Phys. Rev. Lett.*, 109:092501, 2012.
- [11] L.-W. Chen, C. M. Ko, and B.-A. Li. Determination of the stiffness of the nuclear symmetry energy from isospin diffusion. *Phys. Rev. Lett.*, 94:032701, 2005.
- [12] U. Garg. The Giant monopole resonance in the Sn isotopes: Why is tin so 'fluffy'? *Nucl. Phys.*, A788:36–43, 2007.
- [13] A. Klimkiewicz et al. Nuclear symmetry energy and neutron skins derived from pygmy dipole resonances. *Phys. Rev.*, C76:051603, 2007.
- [14] A. Carbone, G. Colo, A. Bracco, L.-G. Cao, P. F. Bortignon, F. Camera, and O. Wieland. Constraints on the symmetry energy and on neutron skins from the pygmy resonances in ^{68}Ni and ^{132}Sn . *Phys. Rev.*, C81:041301, 2010.
- [15] P. Danielewicz and J. Lee. Symmetry Energy I: Semi-Infinite Matter. *Nucl. Phys.*, A818:36–96, 2009.
- [16] D. V. Shetty, S. J. Yennello, and G. A. Souliotis. Density dependence of the symmetry energy and the nuclear equation of state: A Dynamical and statistical model perspective. *Phys. Rev.*, C76:024606, 2007. [Erratum: *Phys. Rev.* C76,039902(2007)].
- [17] B.-A. Li, G.-C. Yong, and W. Zuo. Near-threshold pion production with radioactive beams at the rare isotope accelerator. *Phys. Rev.*, C71:014608, 2005.
- [18] C. Fuchs. Kaon production in heavy ion reactions at intermediate energies. *Prog. Part. Nucl. Phys.*, 56:1–103, 2006.
- [19] C. Hartnack, H. Oeschler, Y. Leifels, E. L. Bratkovskaya, and J. Aichelin. Strangeness Production close to Threshold in Proton-Nucleus and Heavy-Ion Collisions. *Phys. Rept.*, 510:119–200, 2012.
- [20] T. Song, L. Tolos, J. Wirth, J. Aichelin, and E. Bratkovskaya. In-medium effects in strangeness production in heavy-ion collisions at (sub)threshold energies. *Phys. Rev. C*, 103(4):044901, 2021.
- [21] B. Alex Brown. Neutron radii in nuclei and the neutron equation of state. *Phys. Rev. Lett.*, 85:5296–5299, 2000.
- [22] C. J. Horowitz and J. Piekarewicz. Neutron star structure and the neutron radius of Pb-208. *Phys. Rev. Lett.*, 86:5647, 2001.
- [23] C. J. Horowitz and J. Piekarewicz. The Neutron radii of Pb-208 and neutron stars. *Phys. Rev. C*, 64:062802, 2001.
- [24] M. Centelles, X. Roca-Maza, X. Vinas, and M. Warda. Nuclear symmetry energy probed by neutron skin thickness of nuclei. *Phys. Rev. Lett.*, 102:122502, 2009.

- [25] R. A. Hulse and J. H. Taylor. Discovery of a pulsar in a binary system. *Astrophys. J.*, 195:L51–L53, 1975.
- [26] P. Demorest, T. Pennucci, S. Ransom, M. Roberts, and J. Hessels. Shapiro Delay Measurement of A Two Solar Mass Neutron Star. *Nature*, 467:1081–1083, 2010.
- [27] E. Fonseca et al. The NANOGrav Nine-year Data Set: Mass and Geometric Measurements of Binary Millisecond Pulsars. *Astrophys. J.*, 832(2):167, 2016.
- [28] J. Antoniadis et al. A Massive Pulsar in a Compact Relativistic Binary. *Science*, 340:6131, 2013.
- [29] H. T. Cromartie et al. Relativistic Shapiro delay measurements of an extremely massive millisecond pulsar. *Nature Astronomy*, page 439, Sep 2019.
- [30] Z. Arzoumanian. The neutron star interior composition explorer (NICER): mission definition. In *Space Telescopes and Instrumentation 2014: Ultraviolet to Gamma Ray*, volume 9144 of *Proc. SPIE*, page 914420, July 2014.
- [31] P. S. Ray et al. STROBE-X: X-ray Timing and Spectroscopy on Dynamical Timescales from Microseconds to Years. *arXiv e-prints*, page arXiv:1903.03035, March 2019.
- [32] A. L. Watts et al. Dense matter with eXTP. *Sci. China Phys. Mech. Astron.*, 62(2):29503, 2019.
- [33] T. E. Riley et al. A NICER View of PSR J0030+0451: Millisecond Pulsar Parameter Estimation. *Astrophys. J. Lett.*, 887:L21, 2019.
- [34] M. C. Miller et al. PSR J0030+0451 Mass and Radius from *NICER* Data and Implications for the Properties of Neutron Star Matter. *Astrophys. J. Lett.*, 887(1):L24, 2019.
- [35] T. E. Riley et al. A NICER View of the Massive Pulsar PSR J0740+6620 Informed by Radio Timing and XMM-Newton Spectroscopy. *Astrophys. J. Lett.*, 918(2):L27, 2021.
- [36] M. C. Miller et al. The Radius of PSR J0740+6620 from NICER and XMM-Newton Data. *Astrophys. J. Lett.*, 918(2):L28, 2021.
- [37] B. P. Abbott et al. GW170817: Observation of Gravitational Waves from a Binary Neutron Star Inspiral. *Phys. Rev. Lett.*, 119(16):161101, 2017.
- [38] B. P. Abbott et al. Properties of the binary neutron star merger GW170817. *Phys. Rev.*, X9(1):011001, 2019.
- [39] A. Akmal, V. R. Pandharipande, and D. G. Ravenhall. The Equation of state of nucleon matter and neutron star structure. *Phys. Rev.*, C58:1804–1828, 1998.
- [40] R. B. Wiringa, S. C. Pieper, J. Carlson, and V. R. Pandharipande. Quantum Monte Carlo calculations of $A = 8$ nuclei. *Phys. Rev.*, C62:014001, 2000.
- [41] J. Carlson, J. Morales, Jr., V. R. Pandharipande, and D. G. Ravenhall. Quantum Monte Carlo calculations of neutron matter. *Phys. Rev.*, C68:025802, 2003.
- [42] S. Gandolfi, A. Y. Illarionov, K. E. Schmidt, F. Pederiva, and S. Fantoni. Quantum Monte Carlo calculation of the equation of state of neutron matter. *Phys. Rev.*, C79:054005, 2009.

- [43] A. Fabrocini and S. Fantoni. Correlated basis function results for the Argonne models of nuclear matter. *Phys. Lett.*, B298:263–266, 1993.
- [44] B. D. Day. Elements of the Brückner-Goldstone Theory of Nuclear Matter. *Rev. Mod. Phys.*, 39:719–744, 1967.
- [45] B. Ter Haar and R. Malfliet. Nucleons, Mesons and Deltas in Nuclear Matter. A Relativistic Dirac-Brückner Approach. *Phys. Rept.*, 149:207–286, 1987.
- [46] R. Brockmann and R. Machleidt. Relativistic nuclear structure. 1: Nuclear matter. *Phys. Rev.*, C42:1965–1980, 1990.
- [47] W. H. Dickhoff and D. van Neck. *Many-Body Theory EXPOSED! Propagator Description of Quantum Mechanics in Many-Body Systems*. 2005.
- [48] S. K. Bogner, T. T. S. Kuo, and A. Schwenk. Model independent low momentum nucleon interaction from phase shift equivalence. *Phys. Rept.*, 386:1–27, 2003.
- [49] S. R. Beane, W. Detmold, K. Orginos, and M. J. Savage. Nuclear Physics from Lattice QCD. *Prog. Part. Nucl. Phys.*, 66:1–40, 2011.
- [50] N. Ishii, S. Aoki, and T. Hatsuda. The Nuclear Force from Lattice QCD. *Phys. Rev. Lett.*, 99:022001, 2007.
- [51] T. Skyrme. The effective nuclear potential. *Nucl. Phys.*, 9:615–634, 1959.
- [52] J. Decharge and D. Gogny. Hartree-Fock-Bogolyubov calculations with the D1 effective interactions on spherical nuclei. *Phys. Rev.*, C21:1568–1593, 1980.
- [53] J. Boguta and A. R. Bodmer. Relativistic Calculation of Nuclear Matter and the Nuclear Surface. *Nucl. Phys.*, A292:413–428, 1977.
- [54] B. D. Serot and J. D. Walecka. The Relativistic Nuclear Many Body Problem. *Adv. Nucl. Phys.*, 16:1–327, 1986.
- [55] M. Oertel, M. Hempel, T. Klähn, and S. Typel. Equations of state for supernovae and compact stars. *Rev. Mod. Phys.*, 89(1):015007, 2017.
- [56] G. Fiorella Burgio and Anthea F. Fantina. Nuclear Equation of state for Compact Stars and Supernovae. *Astrophys. Space Sci. Libr.*, 457:255–335, 2018.
- [57] R. Engelmann, H. Filthuth, V. Hepp, and E. Kluge. Inelastic Σ -p- interactions at low momenta . *Phys. Lett.*, 21(5):587–589, 1966.
- [58] G. Alexander, U. Karshon, A. Shapira, G. Yekutieli, R. Engelmann, H. Filthuth, and W. Lughofer. Study of the lambda-n system in low-energy lambda-p elastic scattering. *Phys. Rev.*, 173:1452–1460, 1968.
- [59] B. Sechi-Zorn, B. Kehoe, J. Twitty, and R. A. Burnstein. Low-energy lambda-proton elastic scattering. *Phys. Rev.*, 175:1735–1740, 1968.
- [60] J. A. Kadyk, G. Alexander, J. H. Chan, P. Gaposchkin, and G. H. Trilling. Lambda p interactions in momentum range 300 to 1500 mev/c. *Nucl. Phys. B*, 27:13–22, 1971.
- [61] F. Eisele, H. Filthuth, W. Foehlich, V. Hepp, and Gunter Zech. Elastic sigma+ - p scattering at low energies. *Phys. Lett. B*, 37:204–206, 1971.

- [62] I. Vidaña. Hyperons: the strange ingredients of the nuclear equation of state. *Proc. Roy. Soc. Lond.*, A474:0145, 2018.
- [63] L. Fabbietti, V. Mantovani Sarti, and O. Vazquez Doce. Study of the Strong Interaction Among Hadrons with Correlations at the LHC. *Ann. Rev. Nucl. Part. Sci.*, 71:377–402, 2021.
- [64] J. Haidenbauer and U.-G. Meißner. The Julich hyperon-nucleon model revisited. *Phys. Rev.*, C72:044005, 2005.
- [65] T. A. Rijken, M. M. Nagels, and Y. Yamamoto. Baryon-baryon interactions: Nijmegen extended-soft-core models. *Prog. Theor. Phys. Suppl.*, 185:14–71, 2010.
- [66] H. Polinder, J. Haidenbauer, and U.-G. Meißner. Hyperon-nucleon interactions: A Chiral effective field theory approach. *Nucl. Phys.*, A779:244–266, 2006.
- [67] J. Haidenbauer, S. Petschauer, N. Kaiser, U. G. Meißner, A. Nogga, and W. Weise. Hyperon-nucleon interaction at next-to-leading order in chiral effective field theory. *Nucl. Phys.*, A915:24–58, 2013.
- [68] J. Haidenbauer, U. G. Meißner, and A. Nogga. Hyperon–nucleon interaction within chiral effective field theory revisited. *Eur. Phys. J. A*, 56(3):91, 2020.
- [69] <https://inspirehep.net/experiments/1405371?wi-citation-summary=true>.
- [70] <https://www.ub.edu/nplqcd/index.html>.
- [71] B. J. Schaefer, M. Wagner, J. Wambach, T. T. S. Kuo, and G. E. Brown. Low-momentum hyperon-nucleon interactions. *Phys. Rev.*, C73:011001, 2006.
- [72] Y. Fujiwara, Y. Suzuki, and C. Nakamoto. Baryon-baryon interactions in the SU(6) quark model and their applications to light nuclear systems. *Prog. Part. Nucl. Phys.*, 58:439–520, 2007.
- [73] J. Haidenbauer and U.-G. Meißner. A study of hyperons in nuclear matter based on chiral effective field theory. *Nucl. Phys.*, A936:29–44, 2015.
- [74] S. Petschauer, J. Haidenbauer, N. Kaiser, U.-G. Meißner, and W. Weise. Hyperons in nuclear matter from SU(3) chiral effective field theory. *Eur. Phys. J.*, A52(1):15, 2016.
- [75] J. Haidenbauer, U. G. Meißner, N. Kaiser, and W. Weise. Lambda-nuclear interactions and hyperon puzzle in neutron stars. *Eur. Phys. J.*, A53(6):121, 2017.
- [76] D. Logoteta, I. Vidaña, and I. Bombaci. Impact of chiral hyperonic three-body forces on neutron stars. *Eur. Phys. J.*, A55(11):207, 2019.
- [77] D. Gerstung, N. Kaiser, and W. Weise. Hyperon–nucleon three-body forces and strangeness in neutron stars. *Eur. Phys. J. A*, 56(6):175, 2020.
- [78] V. A. Ambartsumyan and G. S. Saakyan. The Degenerate Superdense Gas of Elementary Particles. *Soviet Astronomy*, 4:187, Oct 1960.
- [79] D. Chatterjee and I. Vidaña. Do hyperons exist in the interior of neutron stars? *Eur. Phys. J. A*, 52(2):29, 2016.
- [80] I. Vidaña. Neutron stars and the hyperon puzzle. *EPJ Web Conf.*, 271:09001, 2022.

- [81] I. Bednarek, P. Haensel, J. L. Zdunik, M. Bejger, and R. Manka. Hyperons in neutron-star cores and two-solar-mass pulsar. *Astron. Astrophys.*, 543:A157, 2012.
- [82] S. Weissenborn, D. Chatterjee, and J. Schaffner-Bielich. Hyperons and massive neutron stars: vector repulsion and SU(3) symmetry. *Phys. Rev.*, C85(6):065802, 2012. [Erratum: *Phys. Rev.*C90,no.1,019904(2014)].
- [83] M. Oertel, C. Providência, F. Gulminelli, and Ad R. Raduta. Hyperons in neutron star matter within relativistic mean-field models. *J. Phys.*, G42(7):075202, 2015.
- [84] K. A. Maslov, E. E. Kolomeitsev, and D. N. Voskresensky. Solution of the Hyperon Puzzle within a Relativistic Mean-Field Model. *Phys. Lett.*, B748:369–375, 2015.
- [85] T. Takatsuka, S. Nishizaki, and Y. Yamamoto. Necessity of extra repulsion in hypernuclear systems: Suggestion from neutron stars. *The European Physical Journal A - Hadrons and Nuclei*, 13(1):213–215, Jan 2002.
- [86] T. Takatsuka. Hyperon-mixed neutron stars. *Prog. Theor. Phys. Suppl.*, 156:84–103, 2004.
- [87] I. Vidaña, D. Logoteta, C. Providencia, A. Polls, and I. Bombaci. Estimation of the effect of hyperonic three-body forces on the maximum mass of neutron stars. *EPL*, 94(1):11002, 2011.
- [88] Y. Yamamoto, T. Furumoto, N. Yasutake, and Th. A. Rijken. Multi-pomeron repulsion and the Neutron-star mass. *Phys. Rev.*, C88(2):022801, 2013.
- [89] Y. Yamamoto, T. Furumoto, N. Yasutake, and Th. A. Rijken. Hyperon mixing and universal many-body repulsion in neutron stars. *Phys. Rev.*, C90:045805, 2014.
- [90] D. Lonardonì, A. Lovato, S. Gandolfi, and F. Pederiva. Hyperon Puzzle: Hints from Quantum Monte Carlo Calculations. *Phys. Rev. Lett.*, 114(9):092301, 2015.
- [91] T. Schuerhoff, S. Schramm, and V. Dexheimer. Neutron stars with small radii – the role of delta resonances. *Astrophys. J.*, 724:L74–L77, 2010.
- [92] A. Drago, A. Lavagno, G. Pagliara, and D. Pigato. Early appearance of Δ isobars in neutron stars. *Phys. Rev.*, C90(6):065809, 2014.
- [93] P. Ribes, A. Ramos, L. Tolos, C. Gonzalez-Boquera, and M. Centelles. Interplay between Δ Particles and Hyperons in Neutron Stars. *Astrophys. J.*, 883:168, 2019.
- [94] S. Weissenborn, I. Sagert, G. Pagliara, M. Hempel, and J. Schaffner-Bielich. Quark Matter In Massive Neutron Stars. *Astrophys. J.*, 740:L14, 2011.
- [95] L. Bonanno and A. Sedrakian. Composition and stability of hybrid stars with hyperons and quark color-superconductivity. *Astron. Astrophys.*, 539:A16, 2012.
- [96] T. Klähn, R. Lastowiecki, and D. B. Blaschke. Implications of the measurement of pulsars with two solar masses for quark matter in compact stars and heavy-ion collisions: A Nambu–Jona-Lasinio model case study. *Phys. Rev.*, D88(8):085001, 2013.

- [97] R. Lastowiecki, D. Blaschke, H. Grigorian, and S. Typel. Strangeness in the cores of neutron stars. *Acta Phys. Polon. Supp.*, 5:535–540, 2012.
- [98] J. L. Zdunik and P. Haensel. Maximum mass of neutron stars and strange neutron-star cores. *Astron. Astrophys.*, 551:A61, 2013.
- [99] A. V. Astashenok, S. Capozziello, and S. D. Odintsov. Maximal neutron star mass and the resolution of the hyperon puzzle in modified gravity. *Phys. Rev.*, D89(10):103509, 2014.
- [100] R. H. Dalitz and S. F. Tuan. A possible resonant state in pion-hyperon scattering. *Phys. Rev. Lett.*, 2:425–428, 1959.
- [101] R. H. Dalitz and S. F. Tuan. The energy dependence of low energy K^- -proton processes. *Annals Phys.*, 8:100–118, 1959.
- [102] A. Müller-Groeling, K. Holinde, and J. Speth. K^-N interaction in the meson exchange framework. *Nucl. Phys.*, A513:557–583, 1990.
- [103] J. Haidenbauer, G. Krein, U.-G. Meißner, and L. Tolos. DN interaction from meson exchange. *Eur. Phys. J.*, A47:18, 2011.
- [104] N. Kaiser, P. B. Siegel, and W. Weise. Chiral dynamics and the low-energy kaon - nucleon interaction. *Nucl. Phys.*, A594:325–345, 1995.
- [105] E. Oset and A. Ramos. Nonperturbative chiral approach to s-wave $\bar{K}N$ interactions. *Nucl. Phys.*, A635:99–120, 1998.
- [106] J. A. Oller and U. G. Meißner. Chiral dynamics in the presence of bound states: Kaon nucleon interactions revisited. *Phys. Lett.*, B500:263–272, 2001.
- [107] M. F. M. Lutz and E. E. Kolomeitsev. Relativistic chiral SU(3) symmetry, large N(c) sum rules and meson baryon scattering. *Nucl. Phys.*, A700:193–308, 2002.
- [108] C. Garcia-Recio, J. Nieves, E. Ruiz Arriola, and M. J. Vicente Vacas. $S = -1$ meson baryon unitarized coupled channel chiral perturbation theory and the $S_{(01)}$ - $\Lambda(1405)$ and $-\Lambda(1670)$ resonances. *Phys. Rev.*, D67:076009, 2003.
- [109] D. Jido, J. A. Oller, E. Oset, A. Ramos, and U. G. Meißner. Chiral dynamics of the two $\Lambda(1405)$ states. *Nucl. Phys.*, A725:181–200, 2003.
- [110] B. Borasoy, R. Nissler, and W. Weise. Chiral dynamics of kaon-nucleon interactions, revisited. *Eur. Phys. J.*, A25:79–96, 2005.
- [111] J. A. Oller. On the strangeness -1 S-wave meson-baryon scattering. *Eur. Phys. J.*, A28:63–82, 2006.
- [112] A. Feijoo, V. Magas, and A. Ramos. $S = -1$ meson-baryon interaction and the role of isospin filtering processes. *Phys. Rev.*, C99(3):035211, 2019.
- [113] T. Hyodo and W. Weise. Effective $\bar{K}N$ interaction based on chiral SU(3) dynamics. *Phys. Rev.*, C77:035204, 2008.
- [114] J. Schaffner, J. Bondorf, and I. N. Mishustin. In-medium production of kaons at the mean field level. *Nucl. Phys.*, A625:325–346, 1997.
- [115] K. Tsushima, K. Saito, A. W. Thomas, and S. V. Wright. In-medium kaon and antikaon properties in the quark meson coupling model. *Phys. Lett.*, B429:239–246, 1998. [Erratum: Phys. Lett.B436,453(1998)].

- [116] T. Waas, N. Kaiser, and W. Weise. Effective kaon masses in dense nuclear and neutron matter. *Phys. Lett.*, B379:34–38, 1996.
- [117] M. Lutz. Nuclear kaon dynamics. *Phys. Lett.*, B426:12–20, 1998.
- [118] A. Ramos and E. Oset. The Properties of \bar{K} in the nuclear medium. *Nucl. Phys.*, A671:481–502, 2000.
- [119] L. Tolos, A. Ramos, A. Polls, and T. T. S. Kuo. Partial wave contributions to the anti-kaon potential at finite momentum. *Nucl. Phys.*, A690:547–566, 2001.
- [120] L. Tolos, A. Ramos, and A. Polls. The Anti-kaon nuclear potential in hot and dense matter. *Phys. Rev.*, C65:054907, 2002.
- [121] V. Koch. K^- - proton scattering and the $\Lambda(1405)$ in dense matter. *Phys. Lett.*, B337:7–13, 1994.
- [122] W. Cassing and E. L. Bratkovskaya. Hadronic and electromagnetic probes of hot and dense nuclear matter. *Phys. Rept.*, 308:65–233, 1999.
- [123] C. Hartnack, H. Oeschler, and J. Aichelin. What determines the K^- multiplicity at energies around 1 AGeV - 2 AGeV. *Phys. Rev. Lett.*, 90:102302, 2003.
- [124] W. Cassing, L. Tolos, E. L. Bratkovskaya, and A. Ramos. Anti-kaon production in A+A collisions at SIS energies within an off-shell G matrix approach. *Nucl. Phys.*, A727:59–94, 2003.
- [125] L. Tolos, A. Ramos, and E. Oset. Chiral approach to antikaon s and p-wave interactions in dense nuclear matter. *Phys. Rev.*, C74:015203, 2006.
- [126] L. Tolos, D. Cabrera, and A. Ramos. Strange mesons in nuclear matter at finite temperature. *Phys. Rev.*, C78:045205, 2008.
- [127] D. Cabrera, L. Tolos, J. Aichelin, and E. Bratkovskaya. Antistrange meson-baryon interaction in hot and dense nuclear matter. *Phys. Rev.*, C90(5):055207, 2014.
- [128] D. B. Kaplan and A. E. Nelson. Strange Goings on in Dense Nucleonic Matter. *Phys. Lett.*, B175:57–63, 1986.
- [129] N. Gupta and P. Arumugam. Impact of hyperons and antikaons in an extended relativistic mean-field description of neutron stars. *Phys. Rev. C*, 88(1):015803, 2013.
- [130] V. B. Thapa, M. Sinha, J. J. Li, and A. Sedrakian. Massive Δ -resonance admixed hypernuclear stars with antikaon condensations. *Phys. Rev. D*, 103(6):063004, 2021.
- [131] T. Malik, S. Banik, and D. Bandyopadhyay. Equation-of-state Table with Hyperon and Antikaon for Supernova and Neutron Star Merger. *Astrophys. J.*, 910(2):96, 2021.
- [132] T. Muto, T. Maruyama, and T. Tatsumi. Effects of three-baryon forces on kaon condensation in hyperon-mixed matter. *Phys. Lett. B*, 820:136587, 2021.
- [133] M. F. M. Lutz, C. L. Korpa, and M. Moller. Antikaons and hyperons in nuclear matter with saturation. *Nucl. Phys.*, A808:124–159, 2008.

- [134] D. L. Kaplan et al. A $1.05 M_{\odot}$ Companion to PSR J2222-0137: The Coolest Known White Dwarf? *Astrophys. J.*, 789:119, 2014.
- [135] G. Desvignes et al. High-precision timing of 42 millisecond pulsars with the European Pulsar Timing Array. *Mon. Not. Roy. Astron. Soc.*, 458(3):3341–3380, 2016.
- [136] <https://compose.obspm.fr/>.
- [137] S. Typel et al. CompOSE Reference Manual. *Eur. Phys. J. A*, 58(11):221, 2022.
- [138] V. Dexheimer, M. Mancini, M. Oertel, C. Providência, L. Tolos, and S. Typel. Quick Guides for Use of the CompOSE Data Base. *Particles*, 5(3):346–360, 2022.
- [139] A Li, B. Zhang, N. Bo Zhang, H. Gao, B. Qi, and T. Liu. Internal X-ray plateau in short GRBs: Signature of supramassive fast-rotating quark stars? *Phys. Rev.*, D94:083010, 2016.
- [140] S. Bhattacharyya, I. Bombaci, D. Logoteta, and A. V. Thampan. Fast spinning strange stars: possible ways to constrain interacting quark matter parameters. *Mon. Not. Roy. Astron. Soc.*, 457(3):3101–3114, 2016.
- [141] K. Hebeler, J. M. Lattimer, C. J. Pethick, and A. Schwenk. Equation of state and neutron star properties constrained by nuclear physics and observation. *Astrophys. J.*, 773:11, 2013.
- [142] A. Kurkela, E. S. Fraga, J. Schaffner-Bielich, and A. Vuorinen. Constraining Neutron Star Matter with Quantum Chromodynamics. *Astrophys. J.*, 789(2):127, Jul 2014.